Some Factors Affecting the Size Distributions of Oceanic Bubbles

S. A. THORPE, P. BOWYER, AND D. K. WOOLF

Department of Oceanography, The University, Southampton, United Kingdom

(Manuscript received 23 April 1991, in final form 30 July 1991)

ABSTRACT

The effects of water temperature, dissolved gas saturation levels, and particulate concentrations on the size distribution of subsurface bubbles are investigated using numerical models. The input of bubbles, either at a constant rate in a "steady-state" model or in an initial injection where the development of a bubble "plume" is followed, is kept constant. So too are the model representations of Langmuir circulation and turbulence. An increase in temperature results in a reduction of bubble numbers, a halving at 4-m depth for a 10°C rise in temperature, while an increase in saturation level of 10% increases the bubble concentrations by factors of 3 to 4 at the same depth; the shape of the distribution curves are only slightly modified. The presence of particulates tends to increase the number of small bubbles by inhibiting dissolution.

1. Introduction

In spite of the importance of bubbles in, for example, air–sea gas transfer (Thorpe 1982, 1984a; Memery and Merlivat 1985; Woolf and Thorpe 1991) and sound attenuation (Farmer and Lemmon 1984), there are few direct observations at sea of the size distribution of subsurface bubbles caused by breaking wind waves. Kolovayev (1976), Johnson and Cooke (1979), Mulhearn (1981), and Walsh and Mulhearn (1987) have used cameras to photograph bubbles and measure their sizes, while Medwin (1970, 1977), McDaniel (1988), and Medwin and Breitz (1987) have used acoustic techniques. The results show a strong variation of bubble concentration with the wind speed at which measurements are made, with depth below the surface, and also of the techniques, none of them perfect, used to determine the subsurface distributions. Environmental conditions other than wind speed and temperature have generally been neither reported nor quantified, perhaps because they are often hard to obtain. It is known that bubble size distributions vary considerably from fresh to salt water (Scott 1975) as a consequence of bubbles coalescing more readily when the salinity is small, but as yet there is no direct evidence to demonstrate and quantify the effect of parameters other than wind speed.

Direct and accurate measurements of size distributions are in any case difficult. There is a need to account adequately for the patchy distribution of bubble clouds (for example, see Thorpe 1982; Zedel 1991) when obtaining representative average values, and to avoid bias due to instruments being drawn into regions of convergence, for example, in Langmuir circulation, where higher-than-average populations of bubbles may occur (Thorpe 1984b). However, as measurements are extended to different areas and, especially, in attempting global budgets for gas fluxes or, say, sound generation by resonating bubble clouds, an improved knowledge of the importance of environmental parameters other than wind is desirable—both to gauge the need, or not, to measure bubbles accurately and to provide some account of their likely effects. We have resorted to making some studies using numerical models. These are briefly described in section 2 and the principal results are reviewed in section 3. We examine sensitivity to water temperature (which affects gas solubility, molecular diffusivity and viscosity, and hence bubble dissolution and rise speeds, and so the loss of bubbles at the sea surface), the saturation levels of gases in the water (an important determinant of gas transfer from bubbles), and particulates (which may, by their capture on the surface of bubbles, affect gas transfer and the rise speeds). We shall suppose for our present purpose that these parameters do not change the rate at which bubbles are generated by breaking wind waves—seeking instead to determine only the parameters' effect on the injected bubbles, their mean distributions, and the changes that may occur with time in a single bubble plume.

2. The models

The numerical models are based on that described by Thorpe (1984c) in which the motion of bubbles and the exchange of their gases with the surrounding water are followed in time and space, and to which the reader is referred for details. Bubbles of specified sizes are released into a field of motion resembling Langmuir

Corresponding author address: Prof. Steve A. Thorpe, The University, Department of Oceanography, Southampton, S09 5NH, United Kingdom.

circulation. The buoyant rise of the bubbles and the exchange of gases between each bubble and the surrounding water are represented using formulas describing the terminal rise velocities of bubbles and mass transfer coefficients derived by Levich (1962) and others, as described by Thorpe (1982). Individual bubbles are followed by applying finite-difference forms of these equations in successive time steps, usually of one second. Small-scale turbulence is simulated by adding a component of "random walk." A range of initial sizes of bubbles is introduced to simulate the range produced by breaking waves. The initial distribution, field of motion, and random walk are an ad hoc representation of the injection, advection, and turbulent diffusion of the bubbles.

We carried out two types of numerical experiments: the first seeking a steady-state distribution of bubbles and the second following the evolution of an injected cloud of bubbles. We retained the same input rate, or initial input, of bubbles and looked for variations when

(i) the water temperature was varied from 0° to 20°C,

(ii) the saturation levels of gases dissolved in the water were varied from 90% to 110%, and

(iii) the particulate composition of the seawater is varied from zero to a level some 100 times greater than "typical."

Earlier models have been extended to include bubble capture of particles (see below). The values of viscosity, solubility, and diffusivity at 0°, 10°, and 20°C are given in Table 1.

a. *Steady state*

The results shown in Figs. 1–3 were achieved using an initial distribution of bubbles composed of oxygen and nitrogen in natural atmospheric proportions and with numbers, N, per unit depth and per unit radius of the form

$$\frac{\partial^2 N}{\partial r \partial z} = \begin{cases} N_0 r^{-4}(1 - 2z), & r > 20\ \mu\text{m},\ z < 0.5\ \text{m} \\ 0, & r < 20\ \mu\text{m or } z > 0.5\ \text{m}, \end{cases} \quad (1)$$

TABLE 1. Variation of properties with temperature. Values are for seawater of 35 psu salinity. The diffusivities at 0°C are extrapolated values. Data is taken from Weiss (1970) and Wise and Houghton (1966).

Property	0°C	10°C	20°C
Viscosity (10^{-6} m^2 s^{-1})	1.83	1.39	1.05
Solubility (10^{-6} mol m^{-1} N^{-1})			
(a) Nitrogen	8.062	6.285	5.117
(b) Oxygen	17.49	12.99	10.37
Diffusivity (10^{-9} m^2 s^{-1})			
(a) Nitrogen	1.0	1.8	2.6
(b) Oxygen	1.0	1.7	2.3

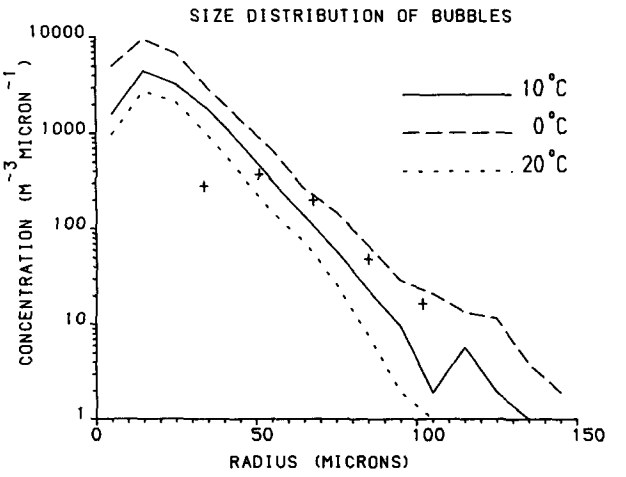

FIG. 1. The mean concentration of bubbles at 4-m depth in the steady-state model plotted on a log scale as a function of radius. The rate of input of bubbles, circulation, and turbulence are constant, the gas saturation level is 100%, and no particles are represented. The curves show the relative concentrations at 0°C (dashed), 10°C (full line), and 20°C (dotted). The crosses show Johnson and Cooke's observations at 4 m in wind speeds of 11–13 m s^{-1}.

where N_0 is a constant (number per unit volume), r is the bubble radius, and z is the depth. This distribution is hypothetical; in justification, various runs with the model have demonstrated that the resulting time-averaged distribution of bubbles is reasonably consistent with the observations of Johnson and Cooke (1979). In any case, any reasonable choice of initial distribution and vertical mixing parameters should be sufficient for an investigation of the kind reported in this paper.

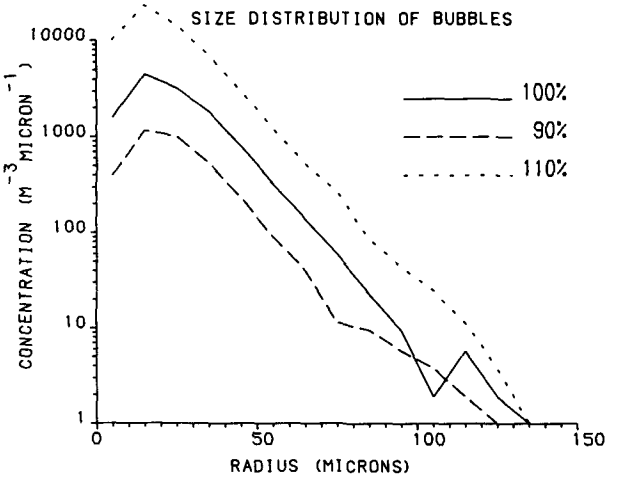

FIG. 2. The mean concentration of bubbles at 4-m depth in the steady-state model plotted on a log scale as a function of radius, as in Fig. 1. Here, however, the water temperature is kept constant at 10°C, no particles are represented, but the gas saturation level in the water is varied. The curves show concentrations at 90% (dashed), 100% (full line, identical to 10°C curve in Fig. 1), and 110% (dotted) saturation levels.

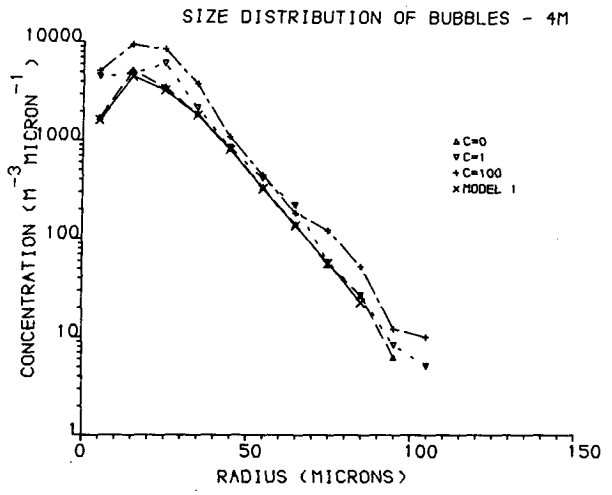

FIG. 3. The mean concentration of bubbles at 4-m depth in the steady-state model plotted on a log scale as a function of radius, as in Fig. 1. Here the temperature and gas saturation levels are kept constant at 10°C and 100%, respectively, but the particulate composition of the water is varied from zero (full curve) to a value (C = 1) similar to that typical in open-ocean conditions (dashed curve) and to a value (C = 100) more typical of coastal waters (dotted curve).

Typically 10 000 bubbles were "injected," with initial radii and depths determined by the probability density function related to (1). A random cross-wind coordinate (i.e., initial horizontal position relative to fixed cells) was selected for each bubble, on the assumption that wave breaking has no positional relation to windrows. Langmuir cells with sinusoidal currents of the type described by Thorpe (1984b) were used with a depth of 10 m, a 20-m spacing between convergence lines, and a maximum downwelling speed of 10 cm s^{-1}, about half the maximum values reported by Weller and Price (1988) in winds of 8–14 m s^{-1}. A random walk every one second corresponding to a depth-independent turbulent diffusion constant of 20 cm^2 s^{-1} was implemented.

Particulates in the water are assumed to have a size distribution that can be described by a power law: $dN/dr = Ar^{-b}$ with $b = 4$ for particulates with $r > 1$ μm, and $b = 2.5$ for particles smaller than this (Hunt 1980). Harris (1977) found a slope of about −2.5 for inorganic particles in the ocean smaller than 1 μm (at depth), and McCave (1975) found a slope of approximately −4 in the spectrum of particulates of $r > 10$ μm near the surface: his spectrum has $A = 10^{16}$. In this case, we choose A to be $C \times 10^{16}$, where C is a concentration factor. The density of the material in the particles smaller than 1 μm is that of seawater, while that of particles larger than this is taken to be 1640 kg m^{-3} at 1 μm decreasing with increasing radius, following McCave (1984). In addition, dissolved organic carbon (DOC) is represented by a separate population of neutrally buoyant particles of radius 1 nm.

Four mechanisms are considered in the capture of particulates by bubbles. 1) Most important for particles of $r > 1$ μm, interception (Weber 1981) is when a particle in a streamline adjacent to the bubble as it rises comes into contact with the bubble surface. 2) Brownian diffusion of particles to the bubble surface (Reay and Ratcliff 1973) is most important for particles of radius < 0.1 μm. 3) Collection by turbulent shear may be more important than other mechanisms for particles of intermediate sizes. 4) Collection by differential settling (Hunt 1980) can be important for rapidly sinking particles and slowly rising bubbles. The attachment efficiency is taken to be unity; all particles coming into contact with the bubble surface adhere to it. Further, no particles are lost from the bubble's surface to the water. The capture of particles representing DOC is supposed to cease when a bubble's surface is covered.

The estimates given above of particle concentration and attachment are subject to much uncertainty. O'Hearn et al. (1988) find Coulter counter measurements of particle concentration to be a factor of 10 less than holographic measurements of similar water samples. Isao et al. (1990) have observed very large (10^3–10^4 times that observed by Harris) populations of fragile, neutrally buoyant particles with radii between 0.1 and 1 μm. Large regional and temporal variations are also likely, for example, between coastal and open-ocean water, and between winter and plankton bloom conditions. The attachment efficiency of particles to particles is quoted in McCave (1983) as about 10%. Wallace and Duce (1978) found that particle flocculation was sensitive to water type.

The state of the surface of the bubble affects the diffusion of gas and particles to and from the bubble, as well as its rise speed and the surface tension. The bubble surface is supposed to be initially clean and hydrodynamically mobile but becomes dirty, and immobile, as organic molecules and particulates diffuse to the surface. This process, and the concomitant reduction in rise speed, have been observed by Detwiler and Blanchard (1978), who found that bubbles became dirty within 5 s of release for bubbles with radii of the order of 0.5 mm. It was found that if the concentration of DOC in the model was set at 70 μg l^{-1}, and a molecular weight of 500 assumed, the model correctly predicted Detwiler and Blanchard's result. The assumed concentration of DOC compares with observed oceanic values of about 500 μg l^{-1} (Duursma 1968). The DOC concentration is specified to be proportional to C, the particle concentration factor. The surface tension falls by 50% when the surface of the bubble becomes dirty. The rise speed of clean bubbles is taken from Thorpe (1982), and for dirty bubbles the data of Clift et al. (1978) is used: this data agrees well with Thorpe's values for dirty bubbles, but is generally applicable over a wider range of radius and density, and so can be applied to aggregates.

D'Arrigo (1986) has observed bubble stabilization by glycopeptide/acyl lipid monolayers. Johnson and

Cooke (1980) observed the stabilization of bubbles on a glass plate associated with thick particulate skins. Johnson and Wangersky (1987) observed stabilization by coatings of hydrophobic particles, and stabilization in crevices in particles has long been known in the field of cavitation research (Hammitt 1980). Medwin (1977) and O'Hern et al. (1988), among others, have observed large populations of bubbles at sea under calm conditions, and there are many observations of long-lived bubbles in tap water (e.g., Gavrilov 1961). The diffusion of gas is assumed to decrease by a factor of $(r_{ag} - r_{air})/r_{air}$, where r_{ag} is the external radius of the aggregate, and r_{air} is the radius of a spherical bubble with the same volume as the free gas within the aggregate, with the proviso that the reduction in diffusion should be no more than 95%. Recognizing that the mechanism of bubble stabilization in the ocean is not known, but assuming some mechanism exists, involving a coating of surface active material (SAM) or particulates, bubbles are assumed to become stable, for the purposes of the model, if $(r_{ag} - r_{air}) > r_{air}$. This criterion is used only to provide quantitative estimates of the production of stable bubbles for the model and has no basis in observation.

b. *A single release*

In order to illustrate the sensitivity of a single bubble "plume" to environmental changes that may affect its detectability by sonar or the collective oscillations of its constituent bubbles, we have introduced a "white" spectrum of 10 000 noninteracting bubbles of 0–200-μm radius uniformly from the surface to 3 m into a flow with $K_V = 100$ cm^2 s^{-1}. The release is in a 2-m-wide zone centered in the downward flow of a Langmuir circulation pattern with, as before, cells 10 m wide and 10 m deep and with a maximum downward flow at 5-m depth of 5 cm s^{-1}. In these numerical experiments we followed the bubbles as before and present histograms of the total bubble numbers remaining in the water at successive times after release.

3. Results and discussion

a. *Steady-state conditions*

The results are illustrated graphically in Figs. 1–3, which show the variations in the bubble size distribution at 4-m depth produced by changes in temperature, gas saturation levels, and particulate composition of the seawater, respectively. The influence of all three parameters is greatest among bubbles at the greatest depth, farthest from the injection zone; a depth of 4 m is a convenient reference level. The concentrations of bubbles (number of bubbles per μm radius) are proportional to their input rates. The average concentrations shown in Figs. 1–3 are calculated for an input rate of 6×10^5 bubbles m^{-2} s^{-1} in the size range 20–500-μm radius, which produces bubble size distributions consistent with Johnson and Cooke (1979) for radii > 60 μm. The precision of the model depends greatly on the number of bubbles followed. Very few bubbles of greater than 100 μm penetrate to a depth of 4 m; the statistics for this part of the curves in Figs. 1 and 2 are correspondingly poor, thus explaining the "noise."

There is some evidence that large (>100-μm radius) bubbles respond differently than do the smaller bubbles to variations in temperature or saturation. (The large bubbles are more sensitive to temperature, but less sensitive to saturation level.) There is, however, no obvious change in shape of the curves shown in Figs. 1 and 2 as temperatures or saturation levels change. The effect of an increase in temperature is to reduce viscosity, decrease solubility, and increase molecular diffusivity by amounts defined in Table 1. Bubbles rise more rapidly as temperature increases due to reduced viscosity. Viscosity also affects gas transfer rates, principally through its effect on bubble rise speed and thus on the Peclet number, $\mathrm{Pe} = wr/D$, where w is the rise speed of a bubble of radius r through the water, and D is the diffusivity of its gas in water. Gas transfer rates increase with increasing Peclet number. The decrease in viscosity with increasing temperature therefore again acts to decrease average bubble concentrations. Solubility and diffusivity also influence gas exchange rates. The rate of gas exchange is approximately proportional to $SD^{2/3}$ (Levich 1962). This varies little with increasing temperature (Table 2); the decrease in solubility, S, with increasing temperature acts to increase the number of bubbles, but this is compensated for by the increase in diffusivity, D. The net effect of temperature change leads to an approximately exponential reduction in the mean bubble concentrations, with a halving for every 10°C rise in temperature at 4-m depth (Fig. 1).

The model results may, in part, explain why the numbers of bubbles with radii less than 100 μm observed by Johnson and Cooke (1979) in seawater at about 2°–3°C were greater than those observed by Walsh and Mulhearn (1987) at a higher temperature of 15°–22°C and at similar wind speeds, but do not explain the differences in the shape of the observed size distributions. (It is possible that water temperature may affect the size and number of bubbles created by breaking waves, but that consideration is beyond the present study.) McDaniel (1988) found no dependence of

TABLE 2. The variation of $SD^{2/3}$, where S is the solubility and D is the diffusivity, with temperature for nitrogen and oxygen. The units are 10^{-12} mol m$^{1/3}$ s$^{-2/3}$ N^{-1}.

	Temperature (°C)		
Gas	0	10	20
N_2	8.06	9.30	9.68
O_2	17.5	18.5	18.1

bubble density on surface water temperature in her analysis of acoustic backscatter data, but comparative information about gas saturation levels does not accompany her dataset.

An increase in gas saturation level enhances the bubble population (Fig. 2). There is an approximately threefold to fourfold increase (more for very small bubbles) at 4-m depth in concentration for every 10% increase in saturation level due to an increased transfer of gas into bubbles, and hence a reduction in the net transfer of gases from bubbles.

The effect of particulates is illustrated in Fig. 3, which shows bubble spectra with particulate concentration factors of 0, 1, and 100. The main difference between the cases $C = 0$ and $C = 1$ is in the concentration of bubbles of radius < 30 μm. For bubbles of radius 5 μm the difference is a factor of 5, and there is no peak for $C = 1$. At this concentration, these bubbles have a heavy organic and particulate coating that acts to reduce the surface tension (and so the Laplacian pressure) as well as the diffusion of gas. For $C = 100$, the concentration of bubbles of radius < 80 μm is greater than in the case of $C = 0$; this difference increases to a factor of about 5 at a radius of 25 μm, but below this radius the concentration again decreases. This decrease is in the numbers of unstabilized bubbles: in the case of such high particle concentrations, most bubbles are stabilized at radii > 15 μm and are then eliminated from the model (otherwise their numbers would grow with time and no "steady rate" would be reached). The trend toward increased bubble numbers with increasing particulate concentration is consistent with McDaniel's (1988) finding of higher bubble numbers in coastal waters. She identified the presence of con-

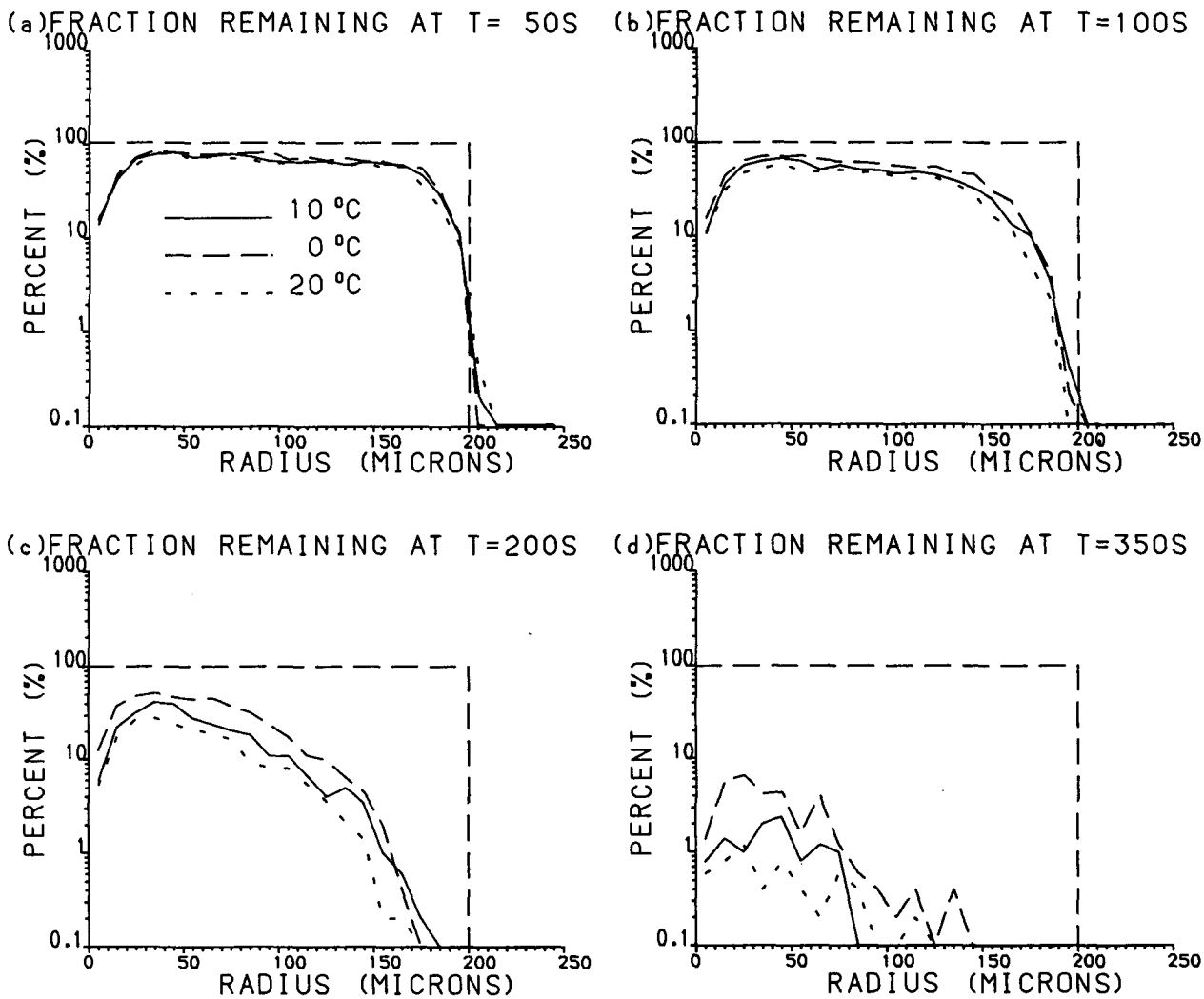

FIG. 4. The number of bubbles surviving until a time, T, after a single release as a fraction of the number of 0–200-μm radius bubbles initially released plotted on a log scale as a function of radius. The initial rectangular distribution is shown. Input, circulation, and turbulence are constant, the gas saturation level is 100%, and no particles are represented. Curves are presented for water temperatures of 0°C (dashed), 10°C (full line), and 20°C (dotted) at four times, T, after release: (a) 50 s, (b) 100 s, (c) 200 s, and (d) 350 s.

taminants, perhaps acting as surfactants or as nuclei for bubble formation, as the likely cause.

b. A single release of bubbles

Bubbles were counted in bins of 10-μm radius from 0 to 250 μm. A total of 10 000 bubbles was released in a uniform distribution from 0 to 200 μm so that there were initially approximately 500 bubbles in each of these bins. The results in Figs. 4–6 are presented as the bubbles remaining as a fraction of 500 in each bin at various times after release (giving a "detection limit" of 0.2%). The initial square distribution is included in each figure segment. Results are presented 50 s, 100 s, 200 s, and 350 s after the release of the bubbles. The bubbles were injected uniformly in the top 3 m and within 1 m of a windrow (the downwelling site).

Bubble rise speed and gas exchange affect the evolution of the bubbles. Most bubbles dissolve in a minute or so, but their lifetimes are much greater in supersaturated water than in subsaturated water. The effect of temperature on rise speeds and gas exchange rates has been described in the previous section. We would again expect bubbles to remain longer in cold water, and this is indeed found (Fig. 4). After 50 s some of the large bubbles have expanded as they rise, "smearing" the large end of the spectrum. Eventually most of the bubbles are lost. Differences in rise speed and gas exchange have a cumulative effect on the distribution as bubbles surface or shrink. The relative effects of temperature (Fig. 4) and saturation level (Fig. 5) changes are similar to those found in the continuous release.

Figure 6 shows the effect of changes in particle concentration, C, on the total number of bubbles. The stable bubbles have here been retained in the model. At 50 s, there is little variation with C for bubbles of

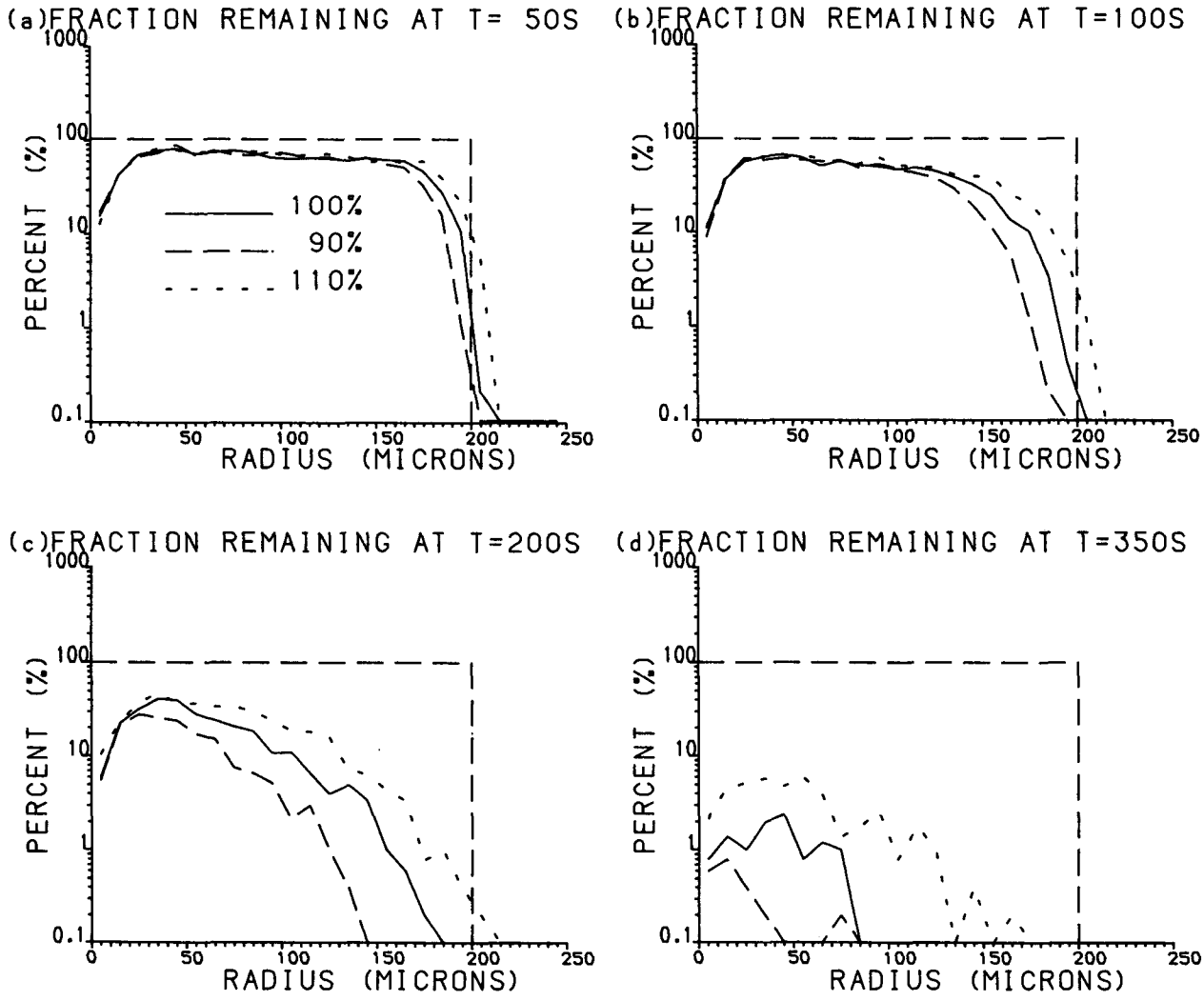

FIG. 5. The fraction of bubble surviving or until a time, T, after a single release plotted on a log scale as a function of radius, as in Fig. 4. The water temperature is kept constant at 10°C and no particles are represented, but the gas saturation level in the water is varied. Curves show the relative concentrations at 90% (dashed), 100% (full line), and 110% (dotted) saturation levels.

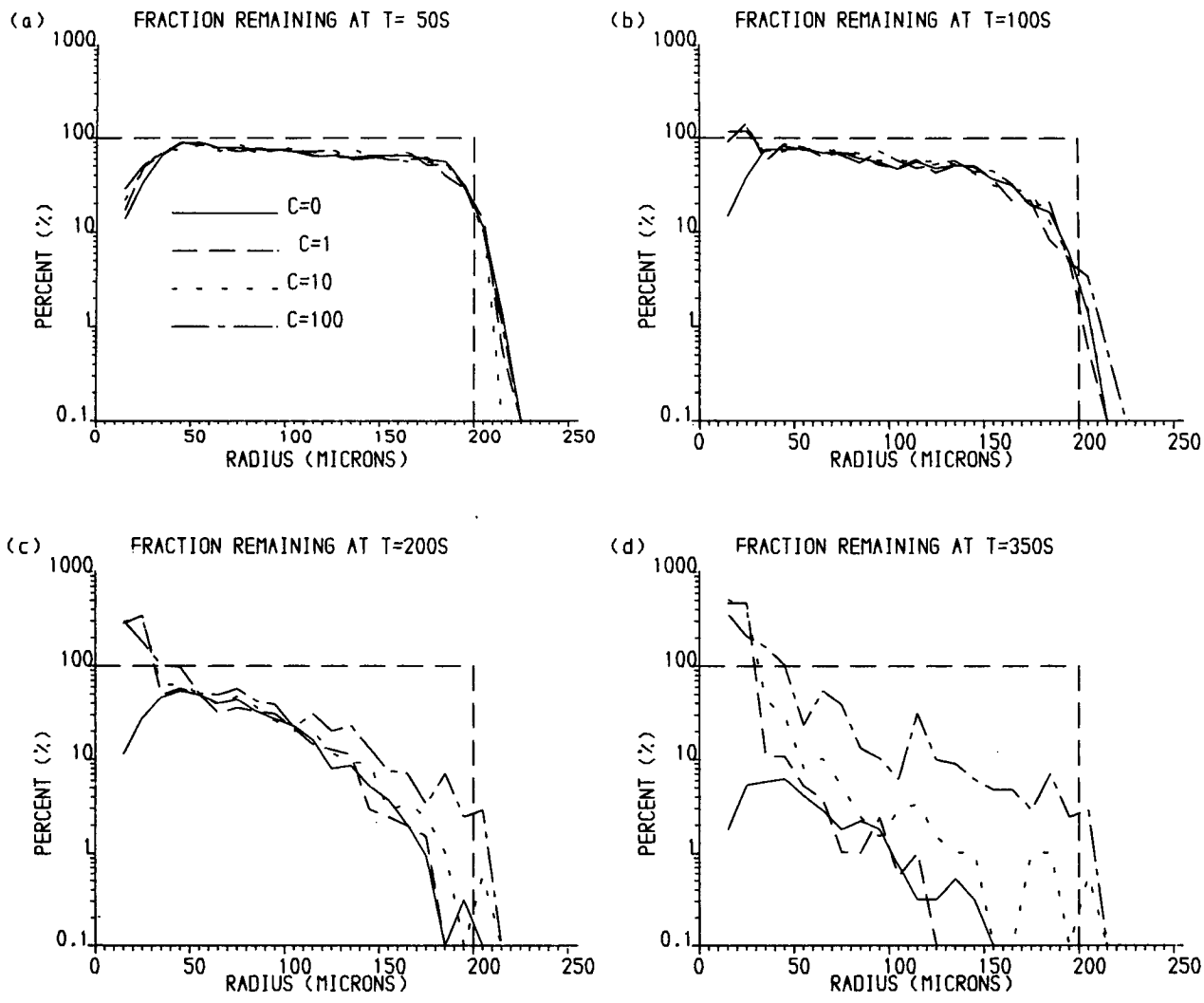

FIG. 6. The fraction of bubbles surviving until a time, T, after a single release plotted on a log scale as a function of radius, as in Fig. 4. The water temperature is 10°C, gas saturation is 100%, and particle concentration factors of 0, 1, 10, and 100 are shown as indicated in part (a) at $T = 50$ s.

radius > 40 μm. Below this radius, the numbers fall off due to the dissolution of the smaller bubbles, most rapidly at $C = 0$. The particulates later cause a significant reduction in diffusion. At 100 s after release, the numbers at $C = 1$, 10, and 100 do not decrease at small bubble radius: larger bubbles that would otherwise have dissolved are stabilized by the compression of their particulate coating. At 350 s, there are very few bubbles left when $C = 0$, but numbers increase with particle concentration. At $C = 100$, the increase is evident over the whole size range, but for $C = 1$ and 10 the increase is only marked at radii < 70 μm. Unlike the size distributions shown in Figs. 4 and 5, there is no peak in the spectrum when the effect of particles is included. At 350 s, most of the bubbles of radii < 40 μm for nonzero C are thickly coated by particulates, and they may perhaps be missed by optical detection techniques, which rely on specular reflections from spherical boundaries. The effect of particulates on high-frequency acoustic scattering from bubbles at near-resonant frequencies will depend on the damping of bubble oscillations caused by the particulates on their surfaces. This is likely to depend on the nature of the particulates themselves.

4. Conclusions

The mean size distribution of subsurface bubbles depends on temperature, gas saturation levels, and particulates in the water. It varies even when the kinematic conditions in the water and bubble injection rates from breaking surface waves are held constant.

Temperature and saturation levels appear to have little effect on the shape of the distributions. The numbers of bubbles beyond the immediate zone of injection appear to vary exponentially with the parameters.

Temperature (Fig. 1) has a fairly small effect, roughly a halving of bubble concentration for every 10°C rise. Saturation (Fig. 2) shows a three- to fourfold increase in concentration for each 10% rise in saturation levels. These effects will change the mean vertical profile of bubble density and void fraction and, for example, the profile of the acoustic scattering cross section per unit volume and influence the bubble-mediated gas transfer between the atmosphere and the ocean. Particulates (Fig. 3) may be an important factor in enhancing the number of smaller bubbles, and this is likely to be a significant factor in coastal waters and perhaps in the open ocean during "bloom" conditions. More deserves to be done, in particular to improve the reliability of the model through improved knowledge of bubble–particulate interactions.

Individual bubble clouds will also be affected by environmental factors (Figs. 4–6), and this needs to be taken into account when estimating, for example, the decreasing void fraction within individual bubble clouds, which may be an important determinant in low-frequency cloud oscillations and their attenuation of underwater sound (Prosperetti 1988).

Acknowledgments. The modeling work reported in this study has been funded by the U.K. Natural Environment Research Council and by a contract from the Ministry of Defence.

REFERENCES

Clift, R., J. R. Grace, and M. E. Weber, 1978: *Bubbles, Drops and Particles.* Academic Press, 380 pp.

D'Arrigo, J., 1986: Stable gas in liquid emulsions. *Studies in Physical Chemistry,* 40, Elsevier, 323 pp.

Detwiler, A., and D. C. Blanchard, 1978: Aging and bursting of bubbles in trace-contaminated water. *Chem. Eng. Sci.,* **33,** 9–13.

Duursma, E. K., 1968: *Chemical Oceanography. Vol. 1.* J. P. Riley and G. Skirrow, Eds. Academic Press, 433–475.

Farmer, D. M., and D. D. Lemmon, 1984: The influence of bubbles on ambient noise in the ocean at high wind speeds. *J. Phys. Oceanogr.,* **14,** 1762–1778.

Fox, F. E., and K. F. Herzfield, 1954: Gas bubbles with organic skin as cavitation nuclei. *J. Acoust. Soc. Amer.,* **26**(6), 984–989.

Gavrilov, L. R., 1969: On the size distribution of gas bubbles in water. *Sov. Phys. Acoust.,* **15,** 22–24.

Hammitt, F. G., 1980: *Cavitation and Multiphase Flow Phenomena.* McGraw Hill, 423 pp.

Harris, J. E., 1977: Characterisation of suspended matter in the Gulf of Mexico—II. Particle rise analysis of suspended matter from deep water. *Deep-Sea Res.,* **77,** 1055–1061.

Hunt, J. R., 1980: Prediction of oceanic particle size distributions from coagulation and sedimentation mechanisms. *Particulates in Water,* M. C. Kavanuagh and J. O. Leckie, Eds., Pergamon, 243–257.

Isao, K., S. Hara, K. Terauchi, and K. Kogure, 1990: Role of submicrometer particles in the ocean. *Nature,* **345,** 242–244.

Johnson, B. D., and R. C. Cooke, 1979: Bubble populations and spectra in coastal waters: A photographic approach. *J. Geophys. Res.,* **84,** 3761–3766.

——, and ——, 1980: Organic particle and aggregate formation resulting from the dissolution of bubbles in seawater. *Limnol. Oceanogr.,* **25,** 653–661.

——, and ——, 1981: Generation of stabilized microbubbles in seawater. *Science,* **213,** 209–211.

——, and P. J. Wangersky, 1987: Microbubbles: Stabilization by monolayers of adsorbed particles. *J. Geophys. Res.,* **92,** 14 641–14 647.

Kolovayev, P. A., 1976: Investigation of the concentration and statistical size distribution of wind produced bubbles in the near-surface ocean layer. *Oceanol.,* **15,** 659–661.

Levich, V. G., 1962: *Physico-chemical Hydrodynamics.* Prentice Hall, 700 pp.

McCave, I. N., 1975: Vertical flux of particulates in the ocean. *Deep-Sea Res.,* **22,** 491–502.

——, 1984: Size spectra and aggregation of suspended particles in the deep ocean. *Deep-Sea Res.,* **31,** 329–352.

McDaniel, S. T., 1988: Acoustical estimates of subsurface bubble densities in the open ocean and coastal waters. *Sea Surface Sound,* B. R. Kerman, Ed., Kluwer Academic, 225–236.

Medwin, H., 1970: In situ acoustic measurements of bubble populations in coastal water. *J. Geophys. Res.,* **75,** 599–611.

——, 1977: In situ acoustic measurements of microbubbles at sea. *J. Geophys. Res.,* **82,** 971–976.

——, and N. B. Breitz, 1989: Ambient and transient bubble spectral densities in quiescent seas and under spilling breakers. *J. Geophys. Res.,* **94,** 12 751–12 759.

Memery, L., and L. Merlivat, 1985: Modelling of gas flux through bubbles at the air–water interface. *Tellus,* **37B,** 272–285.

Mulhearn, P. J., 1981: Distribution of bubbles in coastal waters. *J. Geophys. Res.,* **86,** 6429–6434.

O'Hern, T. J., 1988: Comparisons of holographic and Coulter counter measurements of cavitation nuclei in the ocean. *J. Fluids Eng.,* **110,** 200–207.

Prosperetti, A., 1988: Bubble dynamics in oceanic ambient noise. *Sea Surface Sound,* B. R. Kerman, Ed., Klumer Academic, 151–171.

Reay, D., and G. A. Ratcliffe, 1973: Removal of fine particulates from water by dispersed air floatation. *Can. J. Chem. Res.,* **51,** 178–185.

Scott, J. C., 1975: The role of salt in whitecap persistence. *Deep-Sea Res.,* **22,** 653–657.

Thorpe, S. A., 1982: On the clouds of bubbles formed by breaking wind-waves in deep water, and their role in air-sea gas transfer. *Phil. Trans. Roy. Soc. London,* **A304,** 155–210.

——, 1984a: The role of bubbles produced by breaking waves in super-saturating the near-surface ocean mixing layer with oxygen. *Ann. Geophys.,* **2,** 53–56.

——, 1984b: The effect of Langmuir circulation on the distribution of submerged bubbles caused by breaking waves. *J. Fluid Mech.,* **142,** 151–170.

——, 1984c: A model of the turbulent diffusion of bubbles below the sea surface. *J. Phys. Oceanogr.,* **14,** 841–854.

Wallace, G. T., Jr., and R. A. Duce, 1978: Transport of particulate organic material by bubbles in marine water. *Limnol. Oceanogr.,* **23,** 1155–1167.

Walsh, A. L., and P. J. Mulhearn, 1987: Photographic measurements of bubble populations from breaking wind waves at sea. *J. Geophys. Res.,* **92,** 14 553–14 565.

Weber, M. E., 1981: Collision efficiencies for small particles with a spherical collector at intermediate Reynolds numbers. *J. Separation Process Tech.,* **2,** 29–33.

Weiss, R. F., 1970: The solubility of nitrogen, oxygen and argon in water and seawater. *Deep-Sea Res.,* **17,** 721–735.

Weller, R. A., and J. F. Price, 1988: Langmuir circulation within the oceanic mixed layer. *Deep-Sea Res.,* **35,** 711–747.

Wise, D. L., and G. Houghton, 1966: The diffusion coefficients of ten slightly soluble gases in water at 10–60°C. *Chem. Eng. Sci.,* **21,** 999–1010.

Woolf, D. K., and S. A. Thorpe, 1991: Bubbles and the air–sea exchange of gases in near-saturation conditions. *J. Mar. Res.,* **49,** 435–466.

Zedel, L., and D. Farmer, 1991: Organized structures in subsurface bubble clouds: Langmuir circulation in the open ocean. *J. Geophys. Res.,* **96,** 8881–8900.